Probability of First Passage Failure for Stationary Random Vibration

J. B. ROBERTS*
University of Sussex, Falmer, Brighton, England

For systems responding to stationary random excitation, the problem of calculating the probability, $P(T)$, that first passage failure occurs within an interval of time, 0–T, is considered. By an analysis based on the "in and exclusion" series it is shown that, under certain conditions, $P(T)$ tends to a simple exponential form, as T becomes large. A series expression for the limiting decay rate is deduced. It is demonstrated that the first three terms in the series can be evaluated if the response process is normally distributed, and various methods of estimating the limiting decay rate from these terms are given. In the case of a linear oscillator excited by white noise, numerical results are displayed for a range of critical barrier heights and damping factors, and the analytical estimates of the limiting decay rate are compared with corresponding digital simulation estimates.

I. Introduction

FOR systems responding to random excitation it is important to predict the probability that failure will occur, within a specified time interval. This requires the formulation of a suitable failure criterion. In this paper it will be assumed that failure occurs when the amplitude of the random vibration first exceeds some critical level. This "first-passage" type of failure is of considerable practical importance, since it corresponds to many physical failure mechanisms.

The problem of predicting the probability $P(T)$ that first-passage failure will occur within an interval 0–T is a classical one, of severe analytical difficulty. An exact theoretical solution, in closed form, has not yet been found but recently many approximate solutions have been devised which, together with simulation results, have revealed the essential character of the solution. Crandall has recently compared a number of these approximations.[1] Further approximate theoretical approaches are described in Refs. 2–7.

In this paper attention is focussed on the case where the random vibration is stationary and the mean time to failure is very long compared with the natural period of oscillation of the vibrating system. Clearly, long times to failure are associated with high critical amplitude levels and hence are of most concern in practical applications. Despite the importance of this particular case, comparatively little attention has been given in the literature to the limiting form of $P(T)$, when T is large. A notable exception is the work of Crandall et al.[8] who found that, for a linear oscillator responding to white noise excitation, the distribution of the first passage time tends towards a simple exponential form, as T becomes large. Mark[9] has conjectured that this limiting form can be expected in any situation where the random vibration is stationary.

Here the limiting form of $P(T)$ for large T is examined in some detail, by an analysis based on the "in and exclusion" series.[10] In an earlier paper[11] it was shown that this series can be used to generate a sequence of upper and lower bounds to $P(T)$. Numerical results for a linear oscillator showed that these bounds tend to diverge as T increases. It would appear, therefore, that the series solution can yield little or no information on the behavior of $P(T)$ for large T. However, in a paper of outstanding importance,[12] Kuznetsov et al. have shown that by a suitable transformation of the in and exclusion series it is possible to deduce the limiting form of $P(T)$ for large T. This form turns out to be precisely the exponential form discussed by Crandall et al.[8] and Mark[9]. In addition, from the transformed series, a series expression for the limiting decay rate can be deduced, the first term of which corresponds to the well-known "Poisson crossings" approximation.

In this paper the application of these results to random vibration problems, and in particular to the case of a linear oscillator excited by white noise, is discussed. It is shown that it is possible to evaluate numerically the first three terms in the series expression for the limiting decay rate, if the random vibration is normally distributed. Several methods of estimating the decay rate from these three terms are discussed, including the "nonapproaching points" method described by Stratonovitch.[13] In the case of a linear oscillator it is shown that these methods yield estimates of the decay rate which are reliable when the critical failure amplitude level is high and which also agree closely with simulation estimates at lower critical levels. In particular, it is demonstrated that the general technique is a valuable complement to simulation methods which yield little reliable information for very high critical amplitude levels.

Some work on the application of the transformed "in and exclusion" series to random vibration problems has previously been reported by Lin[6] and Yang and Shinozuka[5]. Lin evaluated the first and second terms in the transformed series for $P(T)$ and discussed various approximations. Numerical results for small values of T were shown which indicate a limiting exponential form for large T. Yang and Shinozuka have used a "point process" approximation to evaluate the first two terms, in the case of narrow-band random vibration, and have discussed various approximations based on these terms. No special attention was paid to the limiting form of $P(T)$.

II. General Series Solution

Consider a random process $X(t)$ which may represent the displacement response of a system to random excitation. Let $P(T)$ be the probability that $X(t)$ crosses some critical level, or barrier, at least once, in a given time interval 0–T. It can be shown[10,11] that

$$P(T) = \sum_{n=1}^{\infty} (-1)^{n+1} \int_0^T \int_{0<t_1<t_2<\ldots<t_n}^T \ldots \int^T p_n(t_1, t_2, \ldots, t_n) \times dt_1\, dt_2 \ldots dt_n \qquad (1)$$

where $p_n(t_1, t_2, \ldots, t_n)\, dt_1\, dt_2 \ldots dt_n$ is the probability that a barrier crossing (from inside to outside) occurs in each of the intervals $dt_1, dt_2, \ldots, dt_n$. Equation (1), known as the "in and exclusion"

Received January 25, 1974; revision received June 21, 1974.
Index categories: Aircraft Vibration; Structural Dynamic Analysis; LV/M Gust Loading and Wind Shear.

* Lecturer in Mechanical Engineering, School of Applied Sciences.

series, is a formal solution to the first passage problem, since the terms in the series can, in principle, be computed. However, the degree of computational effort increases very rapidly with increasing n.[11]

Another serious disadvantage of Eq. (1) is that, for large T, the terms become increasingly large as n increases (in fact the nth term increases as T^n, as $T \to \infty$). At first sight this restricts the use of Eq. (1) to small T values. However, this difficulty can be reduced by recasting Eq. (1) into the following form[12]:

$$P(T) = 1 - \exp\left\{ \sum_{n=1}^{\infty} \frac{(-1)^n}{n!} \int_0^T \int_0^T \cdots \int_0^T g_n(t_1, t_2, \ldots, t_n) \times dt_1\, dt_2 \ldots dt_n \right\} \quad (2)$$

Here the relationships between the g_n and p_n functions can be obtained by expanding the right-hand side of Eq. (2) and comparing the result with Eq. (1).[12]

The g_n functions are symmetric functions of their arguments. For all real processes $X(t)$ with a finite "memory" time, they have the important property that their value falls to zero when the times $t_1, t_2, \ldots, t_n$ are moved apart, i.e.,

$$g_n(t_1, t_2, \ldots, t_n) \to 0$$

provided that at least one difference $t_i - t_j$ of the arguments is increased without limit ($|t_i - t_j| \to \infty$). (This does not apply to the p_n functions, which, under the same conditions, reduce to products of lower order p_n functions.) It is this property of the g_n functions which makes Eq. (2) suitable for the study of $P(T)$ when T is large.

A. Limiting Distribution

Attention will now be focused on the case where $X(t)$ is stationary. Some simplification can then be achieved in the integrals

$$I_n = \int_0^T \int_0^T \cdots \int_0^T g_n(t_1, t_2, \ldots, t_n)\, dt_1\, dt_2 \ldots dt_n \quad (3)$$

which appear in Eq. (2).

For $n = 1$, $g_1(t_1) = \nu$, a constant (equal to the average crossing rate). Clearly

$$I_1 = \nu T \quad (4)$$

For $n = 2$, $g_2(t_1, t_2)$ depends only on the difference between t_1 and t_2. Hence $g_2(t_1 - t_2) = g_2'(\sigma_1)$ where $\sigma_1 = t_1 - t_2$ and

$$I_2 = \int_0^T \int_0^T g_2(t_1, t_2)\, dt_1\, dt_2 = 2 \int_0^T (T - \sigma_1) g_2'(\sigma_1)\, d\sigma_1 \quad (5)$$

This last equation can be generalized. It can be shown that for $n > 2$ (Ref. 12)

$$I_n = \int_0^T (T - \sigma_1) K_n(\sigma_1)\, d\sigma_1 \quad (6)$$

where

$$K_n(\sigma_1) = n(n-1) \int_0^{\sigma_1} \int_0^{\sigma_1} \cdots \int_0^{\sigma_1} g_n'(\sigma_1, \sigma_2, \ldots, \sigma_{n-1}) \times d\sigma_2\, d\sigma_3 \ldots d\sigma_{n-1} \quad (7)$$

Here

$$g_n(t_1, t_2, \ldots, t_n) = g_n'(\sigma_1, \sigma_2, \ldots, \sigma_{n-1}) \quad (8)$$

for a stationary process, where

$$\sigma_i = t_i - t_n \qquad (i = 1, 2, \ldots, n-1) \quad (9)$$

Further simplifications ensue when T is large. Equation (6) can be written in the form

$$I_n = J_n T \{1 - \tau_n / T\} \quad (10)$$

where

$$J_n(T) = \int_0^T K_n(\sigma_1)\, d\sigma_1 \quad \text{and} \quad \tau_n(T) = \frac{1}{J_n} \int_0^T \sigma_1 K_n(\sigma_1)\, d\sigma_1 \quad (11)$$

The integrals $J_n(T)$ and $\tau_n(T)$ will approach asymptotic values $J_n(\infty) = J_n^*$, $\tau_n(\infty) = \tau_n^*$, when T becomes large. τ_n^* are measures of the range of σ_1 over which $K_n(\sigma_1)$ are effectively nonzero. τ_n^* can thus be regarded as a sequence of integral time scales.

It is now necessary to consider two cases: 1) a maximum, finite τ_n^* exists, and 2) τ_n^* increase indefinitely with increasing n (this occurs in the example discussed in Sec. VI). In the first case, if T is very much larger than the maximum τ_n^*, it follows from the previous equations than an appropriate expression for $P(T)$ is as follows:

$$P(T) = 1 - \exp(-\alpha T) \quad (12)$$

where

$$\alpha = \nu - \sum_{n=2}^{\infty} \frac{(-1)^n}{n!} J_n^* \quad (13)$$

will be called the limiting decay rate. In the second case, Eq. (12) is applicable providing the series given by Eq. (2) ultimately converges. For then, a value of n, M say, can be found such that the contribution of terms corresponding to $n > M$ is negligible, and when $T \gg \tau_M^*$ Eq. (12) is valid. When the series diverges, in the second case (this will occur generally at low critical levels), Eq. (12) does not, apparently, represent the limiting form of $P(T)$.

It is interesting to note that it has been rigorously proved by Cramer[14] that, for a normally distributed process, the distribution of crossings is asymptotically Poisson as the critical level (b say) becomes infinitely high, i.e.,

$$P(T) \to 1 - \exp(-\nu T) \quad \text{as} \quad b \to \infty \quad (14)$$

This implies that, for normal processes at least, the summation term in Eq. (13) tends to zero as $b \to \infty$. Equation (13) can, then, be regarded as an expansion for the limiting decay rate, about the limiting Poisson case.

III. Estimation of the Limiting Decay Rate

The computation of J_n for $n > 3$ is prohibitively time consuming. Thus, from Eq. (13)

$$\alpha = \nu[1 - A_2 + A_3 + \text{higher order terms}] \quad (15)$$

where, as will be demonstrated, the nondimensional terms $A_2 = J_2/2\nu$ and $A_3 = J_3/6\nu$ can be computed, if $X(t)$ is normally distributed. In cases where the higher order terms in Eq. (15) are not negligible, a "closure" approximation, based on A_2 and A_3 is required. Three approaches are now discussed.

A. Method of Nonapproaching Points

Stratonovitch has proposed a closure method based on the first two terms in the series solution.[13] This involves replacing the true g_n functions, for $n > 2$, by approximations based on the g_1 and g_2 functions, and leads to the following result:

$$P(T) = 1 - \exp\left\{ \int_0^T \frac{\ln[1 - B(T, \tau)]}{B(T, \tau)} g_1(\tau)\, d\tau \right\} \quad (16)$$

where

$$B(T, \tau) = -\int_0^T \frac{g_2(\tau, u)}{g_1(\tau)} \cdot du \quad (17)$$

For a stationary process, $X(t)$, $g_1(\tau) = \nu$, a constant and $g_2(\tau, u) = g_2'(\tau - u)$, as before. Equation (17) becomes

$$B(T, \tau) = -\frac{1}{\nu} \int_0^T g_2'(\tau - u)\, du \quad (18)$$

If T is very large compared with τ_2^*, $B(T, \tau)$ is virtually independent of τ for all τ values except those very near to the end points of its range, and has the value

$$B(T, \tau) = -\frac{2}{\nu} \int_0^{\infty} g_2'(\sigma)\, d\sigma = -2A_2 \quad (19)$$

It follows that, when T is very large, Eq. (16) reduces to

$$P(T) = 1 - \exp\left\{ -\nu T \left(\frac{\ln[1 + 2A_2]}{2A_2} \right) \right\} \quad (20)$$

This is the same limiting form given by Eq. (12). Here the appropriate limiting decay rate is

$$\alpha/\nu = \ln[1+2A_2]/2A_2 \tag{21}$$

On expanding the log term as a power series, it is found that

$$\alpha/\nu = [1 - A_2 + \tfrac{4}{3}A_2{}^2 - 2A_2{}^3 + \cdots] \tag{22}$$

which agrees with Eq. (15), up to the second term.

B. Euler Transformation

A diverging, or slowly converging, series can often be linearly transformed into a rapidly converging series by a method due to Euler.[15] On applying this transformation to the series expansion for α given by Eq. (15) it is found that

$$\alpha = \nu\{0.5 + (1-A_2)/4 + (1-2A_2+A_3)/8 + \text{higher order terms}\} \tag{23}$$

If the higher order terms in the series of Eq. (15) are significant it can be expected that the transformed series given by Eq. (23) will converge more rapidly.

C. Shanks Transformation

A family of nonlinear transformations for diverging, or slowly converging, series has been extensively discussed by Shanks.[16] The simplest of these (called the e_1 transformation in Ref. 16), when applied to Eq. (15), yields the following result:

$$\alpha = \nu\left\{\frac{A_2 + A_3 - A_2{}^2}{A_2 + A_3} + \text{higher order terms}\right\} \tag{24}$$

For a geometric series the higher order terms in the transformed series of Eq. (24) are zero, and it has been shown by Shanks that they are often very small, even when the original series is only a very rough approximation to a geometric series.

IV. Barrier Configurations

As in Ref. 11, two special types of barrier, which are practically important, will be discussed: the single-sided and double-sided barriers. The single-sided barrier is such that failure occurs when $X(t)$ first exceeds a fixed, constant, critical amplitude level (b say) which may be positive or negative in value. The double-sided barrier is similar except that failure occurs when $|X(t)|$ first exceeds the critical value b.

For simplicity, $X(t)$ will be assumed to have zero mean, and to be symmetric about its mean.

For the single-sided barrier, the appropriate p_n (and hence g_n) functions can be evaluated from the following expression:

$$p_n(t_1, t_2, \ldots, t_n) = \int_0^\infty \int_0^\infty \cdots \int_0^\infty \theta_1\theta_2\ldots\theta_n \times p(b, b, \ldots, b; \theta_1, \theta_2, \ldots, \theta_n)\, d\theta_1\, d\theta_2 \ldots d\theta_n \tag{25}$$

where $p(\xi_1, \xi_2, \ldots, \xi_n; \theta_1, \theta_2, \ldots, \theta_n)$ is the joint density function for $X(t)$ and $\dot{X}(t)$ at the times $t_1, t_2, \ldots, t_n$.

For the double-sided barrier the method of determining the p_n function is similar in principle, but rather more complicated (Ref. 11).

V. Application to Normal Processes

If $X(t)$ is stationary and normally distributed, with zero mean, $p(\xi_1, \xi_2, \ldots, \xi_n; \theta_1, \theta_2, \ldots, \theta_n)$ can be expressed entirely in terms of the covariance of the process $w(\tau)$ as shown in Ref. 11. Thus, from a knowledge of $w(\tau)$, it is possible, in principle, to evaluate the p_n functions [see Eq. (25)] and hence compute the J_n quantities in Eq. (13). In fact the computational work increases very rapidly as n increases and, at present, the computation of J_4 and higher terms is prohibitively time consuming.

A. First Term

The first term in Eq. (13), ν, is the average crossing rate and can be evaluated analytically when $X(t)$ is normal, with zero mean. For a single-sided barrier

$$\nu \propto \exp(-\eta^2/2) \tag{26}$$

and is twice this value for a double-sided barrier.[11] Here the nondimensional critical level

$$\eta = a/\sigma \tag{27}$$

where σ is the standard deviation of $X(t)$.

B. Second Term

To evaluate the second term J_2 (and hence A_2) a combination of analytical and numerical integration is necessary. The first step is to evaluate $g_2'(\sigma_1)$ from the p_2 function and this requires a double integration [see Eq. (25)]. For a normal process with zero mean it is found, after some algebra, that the double integral reduces to the form

$$\Lambda_2 = \int_0^\infty \int_0^\infty \theta_1\theta_2 \exp\{-\delta(\theta_1 - \theta_2) - \gamma\theta_1\theta_2 - \theta_1{}^2 - \theta_2{}^2\} \times d\theta_1\, d\theta_2 \tag{28}$$

where γ and δ can be expressed in terms of $w(\sigma_1)$. Various methods of evaluating this integral have been employed.[11,17,18] Here the technique of Rice and Beer[18] is used, in which θ_1 and θ_2 are transformed to polar coordinates. One integration can then be carried out analytically with the result

$$\Lambda_2 = \int_0^{\pi/4} \frac{\sin\lambda\cos\lambda}{b^2} F_2(c)\, d\lambda \tag{29}$$

where

$$b = 1 + \gamma\sin\lambda\cos\lambda, \quad c = \frac{\delta(\cos\lambda - \sin\lambda)}{2(b)^{1/2}} \tag{30}$$

and

$$F_2(c) = 1 + c^2 + (\pi)^{1/2}\,\mathrm{erf}(c)\, c(\tfrac{3}{2} + c^2)\exp(c^2) \tag{31}$$

The λ integration in Eq. (29), and the subsequent integration of $g_2'(\sigma_1)$ with respect to σ_1, must be performed numerically.

C. Third Term

The method used here to compute J_3 (and hence A_3) is a direct extension of the method described for the second term. For a normal process with zero mean it is first necessary to evaluate a triple integral of the form

$$\Lambda_3 = \int_0^\infty \int_0^\infty \int_0^\infty \theta_1\theta_2\theta_3 \exp\{-\delta_1\theta_1 - \delta_2\theta_2 - \delta_3\theta_3 - \gamma_{12}\theta_1\theta_2 - \gamma_{13}\theta_1\theta_3 - \gamma_{23}\theta_2\theta_3 - \theta_1{}^2 - \theta_2{}^2 - \theta_3{}^2\} \times d\theta_1\, d\theta_2\, d\theta_3 \tag{32}$$

where the γ and δ quantities can be expressed in terms of $w(\sigma_1)$, $w(\sigma_2)$, and $w(\sigma_2 - \sigma_1)$. On transforming to spherical coordinates, one integration can be carried out analytically. Equation (32) then reduces to

$$\Lambda_3 = \int_0^{\pi/2} \int_0^{\pi/2} \frac{\cos^3\phi\sin\phi\sin\lambda\cos\lambda}{b^3} F_3(c)\, d\phi\, d\lambda \tag{33}$$

where

$$\left.\begin{aligned} a &= \delta_1\cos\phi\cos\lambda + \delta_2\cos\phi\sin\lambda + \delta_3\sin\phi \\ b &= 1 + \gamma_{12}\cos^2\phi\sin\lambda\cos\lambda + \gamma_{13}\cos\phi\sin\phi\cos\lambda + \\ &\quad \gamma_{23}\cos\phi\sin\phi\sin\lambda \\ c &= a/2(b)^{1/2} \end{aligned}\right\} \tag{34}$$

and

$$F_3(c) = \left\{1 + \tfrac{9}{4}c^2 + \frac{c^4}{2}\right\} - (\pi)^{1/2}/2[1 - \mathrm{erf}(c)] \times c(\tfrac{15}{4} + 5c^2 + c^4)\exp(c^2) \tag{35}$$

The ϕ, λ integration in Eq. (33), and the subsequent σ_1, σ_2 integration of $g_2'(\sigma_1, \sigma_2)$, must be performed numerically.

VI. Application to the Linear Oscillator

To illustrate the general theory, the case of a linear oscillator, with light viscous damping, subjected to normal, stationary, white noise excitation $n(t)$ with zero mean will now be discussed.

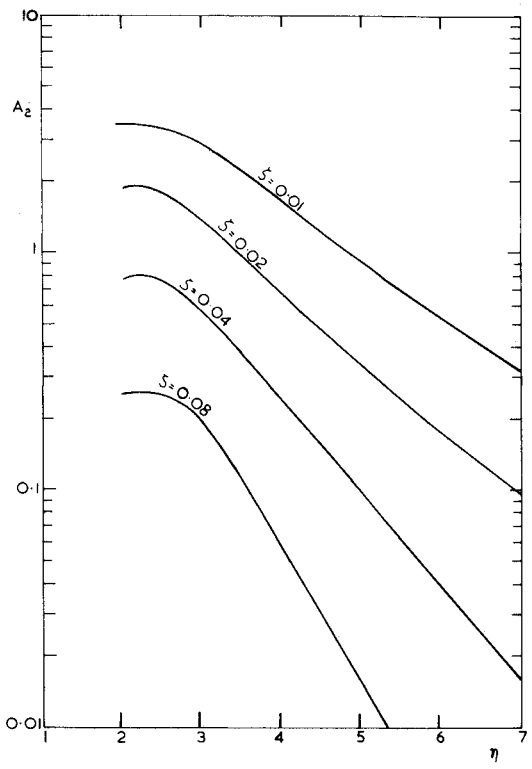

Fig. 1 Variation of A_2 with η for the single-sided barrier, for $\zeta = 0.01$, 0.02, 0.04, and 0.08.

This example is chosen because it is the simplest one which has an engineering significance and also because it is possible to compare the results for this case with the results of other workers.

The appropriate equation of motion is

$$\ddot{X}(t)+2\zeta\omega_0\dot{X}(t)+\omega_0{}^2X(t) = n(t) \tag{36}$$

where ζ is the damping ratio and ω_0 is the undamped natural frequency. $X(t)$ is the displacement response process for the system. From Eq. (36) the covariance function of $X(t)$ is found to be[11]

$$w(\tau) = (1/4\zeta\omega_0{}^3)I_s\exp(-\zeta\omega_0\tau)[\cos\bar{\omega}\tau+(\zeta\omega_0/\bar{\omega})\sin\bar{\omega}\tau] \tag{37}$$

where

$$\bar{\omega} = (1-\zeta^2)^{1/2}\omega_0 \tag{38}$$

and $E\{n(t)n(t+\tau)\} = I_s\cdot\delta(\tau)$. Since $n(t)$ is normal, $X(t)$ is also normal and $w(\tau)$ is a complete statistical description of this process.

In subsequent discussion it is convenient (as in Ref. 11) to replace t by

$$N = \omega_0 t/2\pi \tag{39}$$

i.e., time measured in terms of "natural cycles" of oscillation. $P(N)$, the probability of first passage failure for $X(N)$, depends on η, the nondimensional amplitude and ζ, the damping ratio.

For large N the behavior of $P(N)$ is virtually independent of the initial state of the system and, as the previous analysis indicates, under certain conditions, is of the form

$$P(N) = 1-\exp(-\alpha N) \tag{40}$$

where α is given by Eq. (15). In this paper the variation of α with ζ and η will be examined, for $\eta > 2$ and $0.01 \leqq \zeta \leqq 0.08$.

A. Second Term

The second term A_2 in the series expansion for α given by Eq. (15) can be evaluated by the technique described in Sec. V-B, using the covariance function given by Eq. (37). Figures 1 and 2 show the computed variation of A_2 with η for the single-sided and double-sided barriers, respectively. In both cases, results are shown for $\zeta = 0.01$, 0.02, 0.04, and 0.08.

A significant feature of these results is that, given values of ζ and η. A_2 for a single-sided barrier is virtually identical in value to A_2 for a double-sided barrier with the same η, but with double

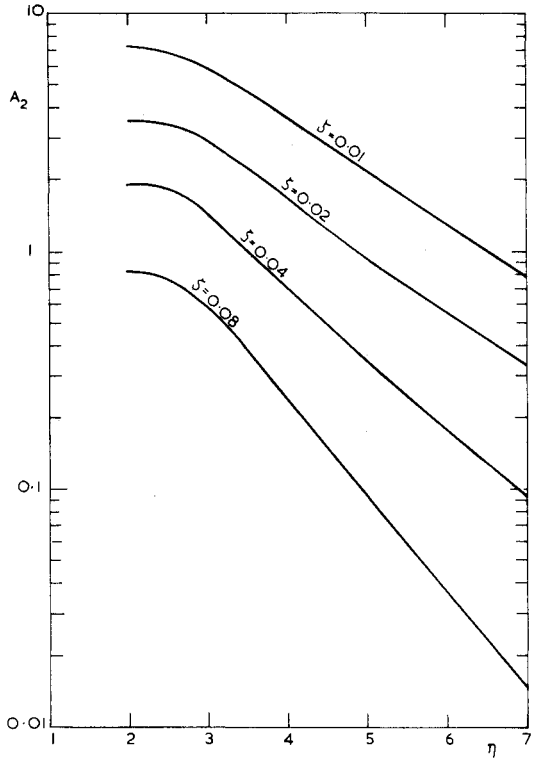

Fig. 2 Variation of A_2 with η for the double-sided barrier, for $\zeta = 0.01$, 0.02, 0.04, and 0.08.

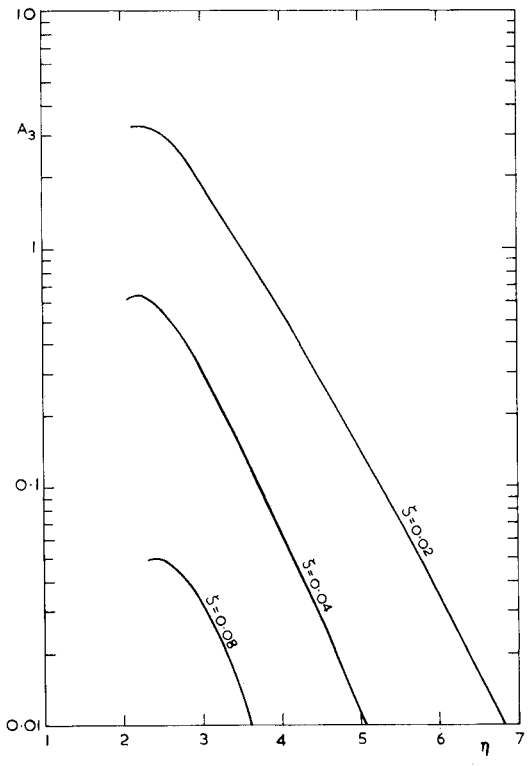

Fig. 3 Variation of A_3 with η for the single-sided barrier, for $\zeta = 0.02$, 0.04, and 0.08.

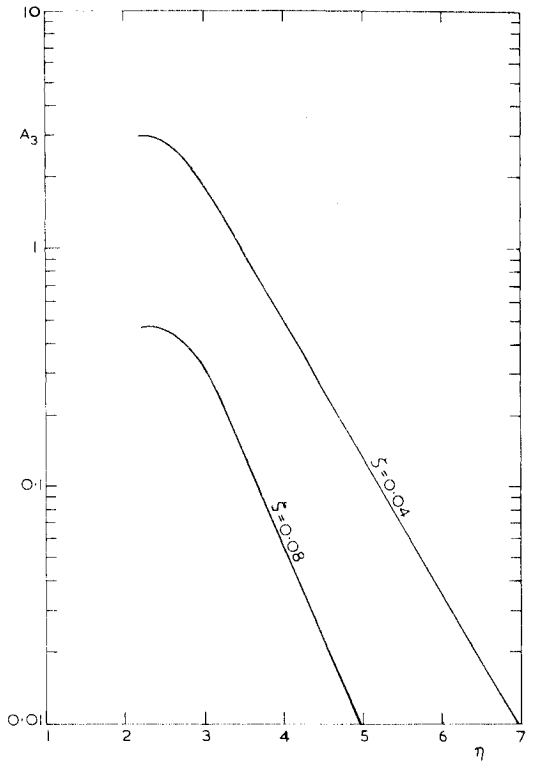

Fig. 4 Variation of A_3 with η for the double-sided barrier, for $\zeta = 0.04$, and 0.08.

the value of ζ. For example, the curve in Fig. 1 for $\zeta = 0.02$ is virtually identical to the curve in Fig. 2 for $\zeta = 0.04$. This implies that the values of A_2 for a double-sided barrier can be deduced from the results for a single-sided barrier.

B. Third Term

The third term A_3 in Eq. (15) can be computed by the method given in Sec. V-C. Figures 3 and 4 show the variation of A_3 and η for the single-sided and double-sided barriers, respectively. In Fig. 3 curves are shown for $\zeta = 0.02$, 0.04, and 0.08 while in Fig. 4, curves for $\zeta = 0.04$ and 0.08 are shown. Results for smaller damping factors have not been calculated, although there is no obstacle other than the long computer time required.

It will be observed that the curve for $\zeta = 0.04$ in Fig. 3 bears a close resemblance to that for $\zeta = 0.08$ in Fig. 4; this feature is parallel to that observed in the results for A_2. However, in the case of A_3, the two aforementioned curves are only equal in a very rough sense.

C. Correlation Time Scales τ_n^*

Figure 5 shows the variation of τ_2^* (in cycles) with η, for various ζ, in the case of a single-sided barrier. This shows, as one might expect, that this time scale decreases with increasing η, and with increasing ζ. For the narrow-band case considered here ($\zeta < 0.1$), and a single-sided barrier, $g'_2(\sigma_1)$ peaks at integer multiples of one cycle, with the first peak contributing most to J_2^*. As η increases the first peak in $g'_2(\sigma_1)$ becomes predominant and clearly τ_2^* will approach a value of one cycle, as shown in Fig. 5. Similarly, for the double-sided barrier, the value of τ_2^* will approach one half cycle as η becomes large.

Figure 6 shows the variation of τ_3^* (in cycles) with η for various ζ, in the case of a single-sided barrier. The characteristics of τ_3^* are evidently similar to τ_2^*, but the over-all magnitude level of τ_3^* is higher, by a factor of about two. Since the predominant peak of $g'_3(\sigma_1, \sigma_2)$ occurs at $\sigma_1 = 2$, $\sigma_2 = 1$, it follows that τ_3^* will approach a value of two cycles when η is large, as shown in Fig. 6. Similarly, for the double-sided barrier, τ_3^* will approach a value of one cycle, as η becomes large.

Although τ_n^* cannot be evaluated for $n > 3$, it can be inferred, by reasoning similar to that given previously for τ_2^* and τ_3^*, that when η is large τ_n^* will approach a value of n cycles, in the case of a single-sided barrier, whereas for a double-sided barrier τ_n^* will approach a value of $n/2$ cycles. Thus the present problem falls into the second category discussed in Sec. II-A, and the validity of Eq. (40) can only be proved to hold when the series solution converges. Since the convergence, or otherwise, of the series solution cannot be definitely established, but only inferred, from the magnitude of A_2 and A_3 the behavior of $P(N)$ has also been studied by a separate approach, based on digital simulation.

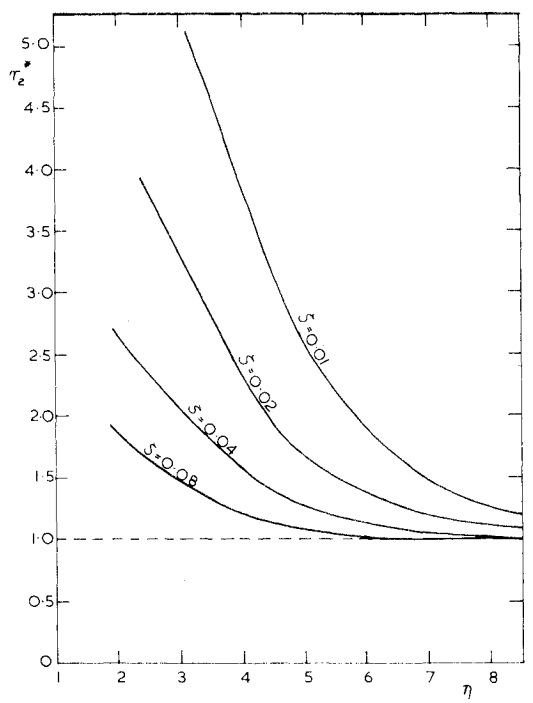

Fig. 5 Variation of τ_2^* (in cycles) with η for the single-sided barrier, for $\zeta = 0.01$, 0.02, 0.04, and 0.08.

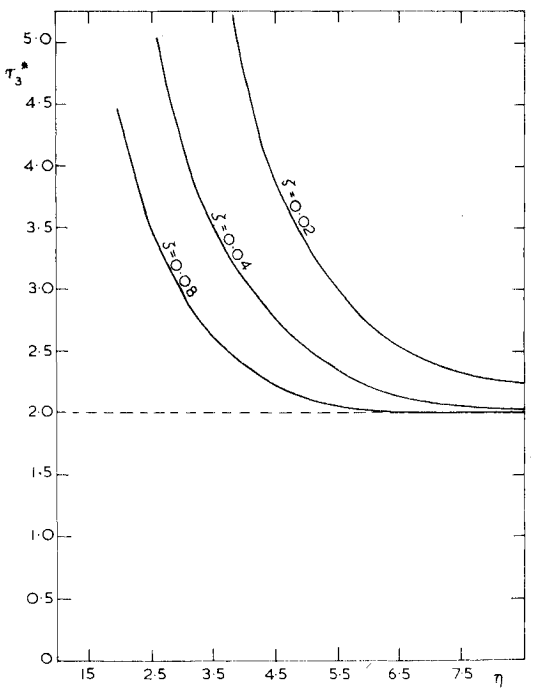

Fig. 6 Variation of τ_3^* (in cycles) with η for the single-sided barrier, for $\zeta = 0.02$, 0.04, and 0.08.

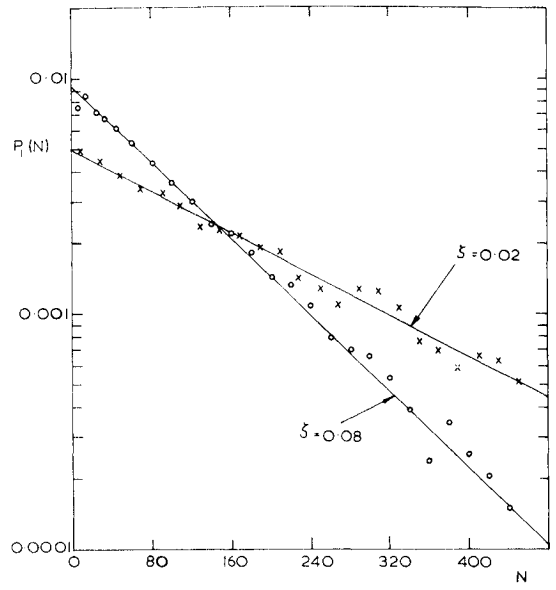

Fig. 7 Simulation estimates of the variation of $p_1(N)$ with N for the single-sided barrier, for $\eta = 3$, $\zeta = 0.02$ and 0.08.

D. Simulation Work

The applicability of Eq. (40) has been examined by a comparison with digital simulation results[8] for $0.01 \leqq \zeta \leqq 0.08$ and various values of η. Similar simulation work has been carried out by the author, using the technique described in an earlier work.[19]

For this purpose it is convenient to examine the first passage density function

$$p_1(N) = dP(N)/dN \tag{41}$$

If Eq. (40) is valid then, from Eq. (41)

$$p_1(N) = \alpha \exp(-\alpha N) \qquad \text{for large } N \tag{42}$$

and (at least for large N) it should be possible to draw a straight line through simulation estimates of $p_1(N)$, if these are plotted against N on a log-linear graph. If Eq. (42) represents $p_1(N)$ over a sufficiently large range of N, then the mean first passage time $\bar{N}$ can be estimated from

$$\bar{N} = \int_0^\infty N p_1(N)\, dN = \frac{1}{\alpha} \tag{43}$$

Figure 7 shows typical simulation estimates for $p_1(N)$, as a function of N, for the single-sided barrier, with $\eta = 3$ and $\zeta = 0.08$ and 0.02. For $\zeta = 0.08$, 10,000 samples of the first passage time were generated, using the method of Ref. 19, while for $\zeta = 0.02$, 5000 samples were generated. The straight lines which have been drawn through the estimates were obtained from Eq. (42), using $\alpha = 1/\hat{\bar{N}}$, where $\hat{\bar{N}}$ is the simulation estimate of the mean first passage time [see Eq. (43)]. These results support the findings of Crandall et al., who concluded that for high barrier levels Eqs. (42) and (43) together provide a good description of $p_1(N)$, except when N is very small.[8]

It is interesting to note, from Figs. 1, 3, 5, and 6 that, for $\eta = 3$, A_2, A_3, $\tau_2{}^*$, and $\tau_3{}^*$ are as given in Table 1. In the case $\zeta = 0.08$, A_2 and A_3 indicate a rapid convergence of the series solution and thus, when $N \gg 3$ the analysis given earlier indicates that Eqs. (42) and (43) are valid. This conclusion is strongly supported by the results in Fig. 7. For $\zeta = 0.02$, A_2 and A_3 indicate a fairly rapid divergence of the series solution, but nevertheless the result shown in Fig. 7 indicates that Eqs. (42) and (43) are still satisfactory. This may be an indication that the series solution does ultimately converge.

Table 1 Variations with η for the single-sided barrier

ζ	A_2	A_3	$\tau_2{}^*$	$\tau_3{}^*$
0.08	0.182	0.032	1.47	3.01
0.02	1.36	2.05	3.40	6.75

In the comparison between theoretical and simulation estimates of α, given in Sec. VI-E, the simulation estimates have been obtained by simply taking the reciprocal of $\hat{\bar{N}}$ [see Eq. (43)] and in each case 1000 samples were used to find $\hat{\bar{N}}$. With the assumption that Eq. (42) is valid, confidence limits can be established for the α estimates. If $\hat{\alpha}$ is an estimate of α, found from 1000 crossings, there is a roughly 95% probability that α lies in the range $(1 \pm 0.063)\,\hat{\alpha}$.

E. Estimation of the Limiting Decay Rate

Figure 8 shows estimates of the variation of α/ν with η for $\zeta = 0.08$ and for both single-sided and double-sided barriers. In both cases simulation estimates are shown for $\eta = 2.5$, 3, and 3.5, together with the appropriate 95% confidence limits. The broken lines, labelled S_2 and S_3, are the partial sums of the series solution given by Eq. (15), (i.e., $S_2 = 1 - A_2$, $S_3 = 1 - A_2 + A_3$). The chain dotted lines represent the nonapproaching points estimates (hence referred to as NAP estimates) obtained from A_2 [see Eq. (12)]. The full lines are obtained from the first term of the Shanks transformation (hence referred to as Shanks estimates) in Eq. (24), i.e.,

$$\alpha/\nu = (A_2 + A_3 - A_2{}^2)/(A_2 + A_3) \tag{44}$$

The broken line (with long dashes) shows the estimated variations of α with η, obtained from the sum of the first three terms in Eq. (23) (hence referred to as the Euler estimate).

It is apparent from Fig. 8 that, for a given η, the convergence of the series solution is most rapid in the case of a single-sided barrier. For this barrier the NAP and Shanks estimates are in close agreement with each other, and with the simulation results. For the double-sided barrier, at low η the convergence of the series solution is slow and there is a large difference between S_2 and S_3. Despite this, the NAP and Shanks estimates are in close mutual agreement, and in good agreement with the simulation estimates. The Euler estimate for this case agrees very closely with the Shanks estimate at low η, but diverges at high η. The reason for this is that Eq. (23) only converges more rapidly than

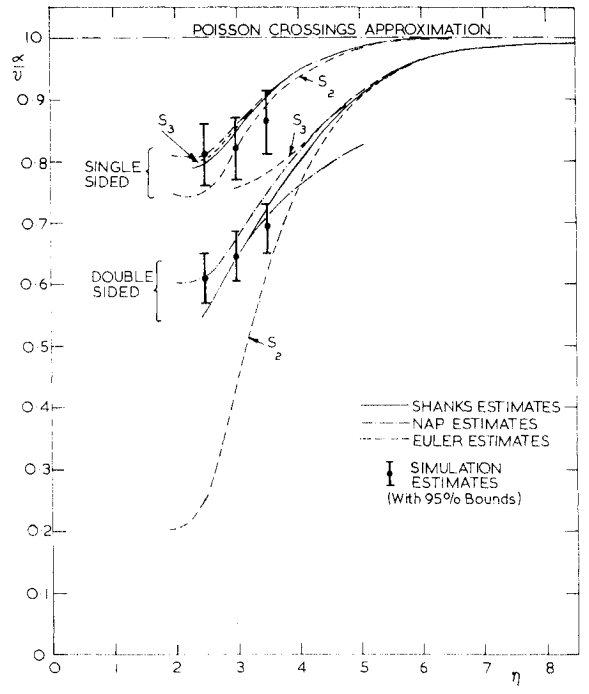

Fig. 8 Variation of α/ν with η for the single and double-sided barriers, $\zeta = 0.08$.

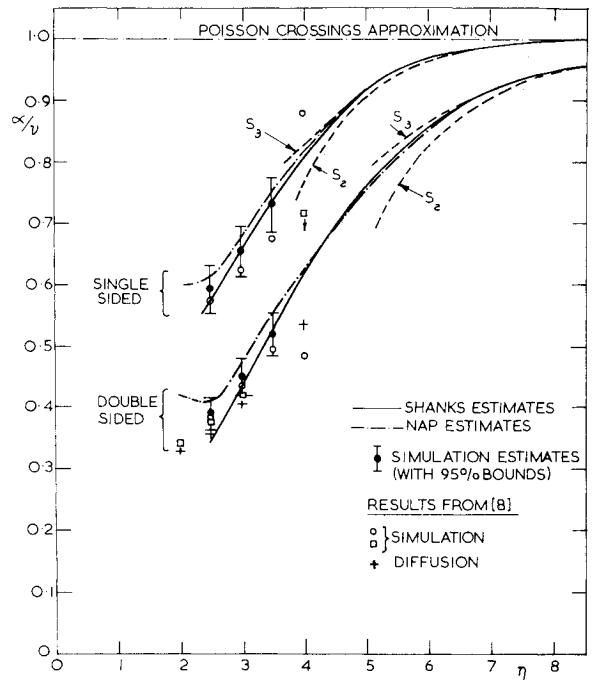

Fig. 9 Variation of α/ν with η for the single and double-sided barriers, $\zeta = 0.04$.

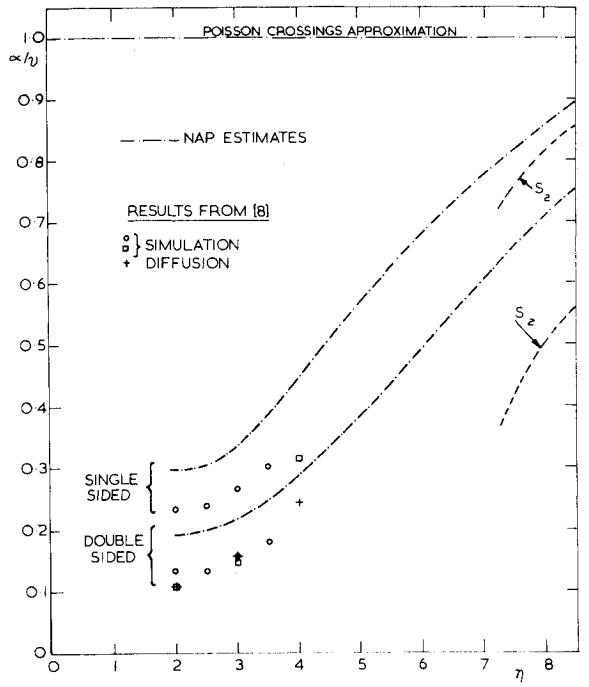

Fig. 11 Variation of α/ν with η for the single and double-sided barriers, $\zeta = 0.01$.

Eq. (15) when the latter is very slowly convergent, or divergent. Thus, for high η, where the original series converges rapidly, the higher order terms in Eq. (23) are significant and the Euler estimate is appreciably in error. For both barriers, the series solution is rapidly convergent in the region $0.8 < (\alpha/\nu) \leqq 1.0$, enabling the accuracy and range of validity of the simple "Poissons crossings" approximation to be accurately assessed.

Figure 9 shows a similar comparison of various estimates of α, for $\zeta = 0.04$. Here the Euler estimate has been omitted (it agrees very closely with Shanks estimates at low η) and only the upper parts of the S_2 and S_3 curves are shown. In this figure are also shown the estimates of α obtained by Crandall et al.[8] by digital simulation and by a numerical diffusion method. It should be noted that at $\eta = 4$ the estimates from Ref. 8 have a high degree of potential error. Bearing this in mind, the agreement between the NAP, Shanks, and simulation estimates is very encouraging. The available evidence suggests that, for both barriers, the Shanks estimate is slightly better than the NAP estimate. It is noted that the single-sided barrier results for $\zeta = 0.04$ agree, very closely, with the double-sided barrier results for $\zeta = 0.08$. This can be anticipated from the characteristics of the A_2 and A_3 terms, discussed in Secs. VI-A and VI-B.

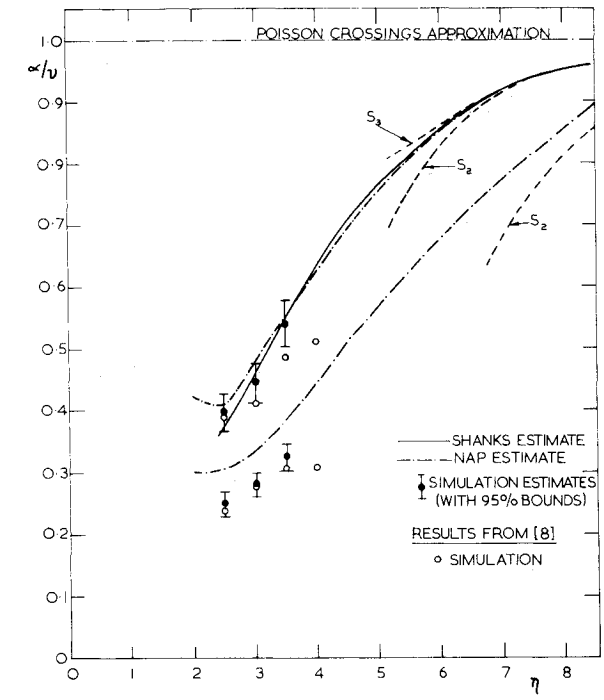

Fig. 10 Variation of α/ν with η for the single and double-sided barriers, $\zeta = 0.02$.

In Fig. 10 a similar comparison of various estimates is shown, for $\zeta = 0.02$. Here the NAP estimates are shown for both types of barrier, but the Shanks estimates are shown only for the single-sided barrier (the A_3 terms has not been computed for the double-sided barrier). For the single-sided barrier the NAP and Shanks estimates are again in close mutual agreement, and in fairly good agreement with the simulation estimates. For the double-sided barrier, the NAP estimate appears to be slightly too high but nevertheless is remarkably good when the divergence of the series solution, at low η, is taken into account. Thus, at $\eta = 3$, $A_2 = 2.89$, indicating a very rapid divergence in this case, and yet the NAP estimate ($\alpha/\nu = 0.335$) agrees with the simulation estimates ($\alpha/\nu = 0.275$) within about 20%. Of course, at higher values of η, the series solution is convergent and, in view of the previous results, one can expect the accuracy of the NAP approximation to improve. It is noted that the single-sided results for $\zeta = 0.02$ agree very closely with the double-sided results for $\zeta = 0.04$.

Finally, in Fig. 11, a corresponding comparison is shown for $\zeta = 0.01$. Here the NAP estimates, the two barrier types, are compared with estimates obtained by Crandall et al.[8] Again, taking the rapid divergence of the series solution, at low η, into account, the agreement between the NAP estimates and the results from Ref. 8 is remarkably good. It is noted that the single-sided results of $\zeta = 0.01$ agree very closely with the double-sided results for $\zeta = 0.02$.

VII. Effect of Initial Conditions

So far, only the asymptotic behavior of $P(N)$, for large N, has been discussed. This limiting behavior is independent of initial

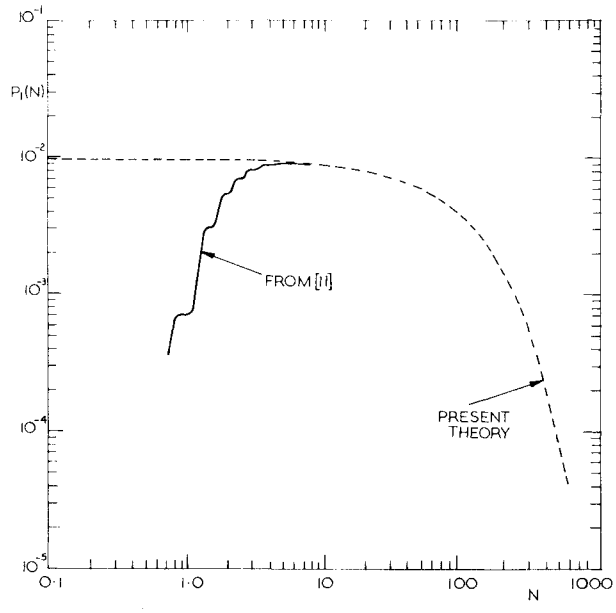

Fig. 12 Variation of $p_1(N)$ with N for the single-sided barrier, $\eta = 3$ and $\zeta = 0.08$.

conditions. In an earlier paper,[11] the initial behavior of $P(N)$ was discussed, for the case of a "zero start" (i.e., system initially at rest), and numerical results for small N were obtained for the linear oscillator, by evaluating the first three terms in Eq. (1). It is interesting to examine, therefore, the extent to which the previously obtained results for small N match with the results for large N, given here.

Figure 12 shows a typical comparison for the linear oscillator case. Here, the barrier is of the single-sided type and $\zeta = 0.08$, $\eta = 3$. The full line in the figure shows the variation of $p_1(N)$ with N obtained by applying a Shanks transformation to the first three terms in Eq. (1) (see Fig. 10 in Ref. 11). The broken line shows the asymptotic solution for this case, given by Eq. (46), where $\alpha/\nu = 0.84$ (see Fig. 8) is the Shanks estimate obtained from A_2 and A_3. Clearly, the two solutions match very satisfactorily at $N \sim 10$, giving the entire $p_1(N) - N$ variation.

VIII. Conclusions

The main conclusions of this paper are summarized as follows.

1) For stationary random vibration, it is possible to deduce from the "in and exclusion" series the limiting form of the distribution of the first passage time $P(N)$, for large N. This form is given by $P(N) = 1 - \exp(-\alpha N)$ where α, the limiting decay rate, can be expressed as a series.

2) For normal processes, the first three terms in the series expression for α can be evaluated. These terms enable a variety of estimates of α to be made.

3) In the case of a linear oscillator excited by white noise, the theoretically obtained estimates of α agree well with each other and with simulation estimates. In particular, the nonapproaching points estimates, which require only the first two terms in the series for α and are thus the easiest to compute, are fairly accurate for $\eta > 3$ and $0.01 \leq \zeta \leq 0.08$, the largest errors occurring in the low end of the ζ range.

4) For the linear oscillator case, the variation of α/ν with η for a single-sided barrier with $\zeta = \zeta^1$ (say) is virtually identical to the variation of α/ν with η for a double-sided barrier, with $\zeta = 2\zeta^1$ (over the range of η and ζ studied).

5) By combining the analysis given in Ref. 11 for the initial, "transient" behavior of $P(N)$ with the asymptotic analysis given here, the variation of $P(N)$ with N, over the entire range of N, can, for engineering purposes, be satisfactorily estimated.

References

[1] Crandall, S. H., "First-Crossing Probabilities of the Linear Oscillator," *Journal of Sound and Vibration*, Vol. 12, 1970, pp. 285–299.

[2] Toland, R. H. and Yang, C. Y., "Random Walk Model for First-Passage Probability," *Transactions of the ASCE, Journal of the Engineering Mechanics Division*, Vol. 97, EM3, 1971, pp. 791–807.

[3] Shipley J. W. and Bernard, M. C., "The First-Passage Time Problem for Simple Structural Systems," *Transactions of the ASME, Journal of Applied Mechanics*, Vol. 39, 1972, pp. 911–917.

[4] Yang, J. N. and Shinozuka, M., "On the First-Excursion Probability in Stationary Narrow-Band Random Vibration," *Transactions of the ASME, Journal of Applied Mechanics*, Vol. 38, 1971, pp. 1017–1022.

[5] Yang, J. N. and Shinozuka, M., "On the First-Excursion Probability in Stationary Narrow-Band Random Vibration II," *Transactions of the ASME, Journal of Applied Mechanics*, Vol. 39, 1972, pp. 733–738.

[6] Lin, Y. K., "First-Excursion Failure of Randomly Excited Structures," *AIAA Journal*, Vol. 8, No. 4, April 1970, pp. 720–725.

[7] Lin, Y. K., "On First-Excursion Failure of Randomly Excited Structures: II," *AIAA Journal*, Vol. 8, No. 10, Oct. 1970, pp. 1888–1890.

[8] Crandall, S. H., Chandiramani, K. L., and Cook, R. G., "Some First Passage Problems in Random Vibration," *Transactions of the ASME, Journal of Applied Mechanics*, Vol. 33, 1966, pp. 532–538.

[9] Mark, W. D., "On False-Alarm Probabilities of Filtered Noise," *Proceedings of the IEEE*, Vol. 54, 1966, pp. 316–317.

[10] Rice, S. O., "Mathematical Analysis of Random Noise," *Bell System Technical Journal*, Vol. 24, 1945, pp. 46–156.

[11] Roberts, J. B., "An Approach to the First-Passage Problem in Random Vibration," *Journal of Sound and Vibration*, Vol. 8, 1968, pp. 301–328.

[12] Kuznetsov, P. I., Stratonovitch, R. L., and Tikhonov, V. I., "On the Duration of Excursions of Random Functions," *Zhurnal Tekhnicheskoi Fiziki*, Vol. 24, 1954, pp. 103–124; translated in *Non-Linear Transformations of Stochastic Processes*, Pergamon Press, New York, 1965, pp. 341–353.

[13] Stratonovitch, R. L., *Topics in the Theory of Random Noise*, Vol. 1, Gordon and Breach, New York, 1963, pp. 143–176.

[14] Cramer, H., "On the Intersections between the Trajectories of a Normal Stationary Stochastic Process and a High Level," *Arkiv for Matematik*, Vol. 6, 1966, pp. 337–349.

[15] Van Dyke, M., *Perturbation Methods in Fluid Mechanics*, Academic Press, New York, 1964, pp. 202–210.

[16] Shanks, D., "Non-Linear Transformations of Divergent and Slowly Convergent Sequences," *Journal of Mathematics and Physics*, Vol. 34, 1955, pp. 1–42.

[17] Tikhonov, V. I., "The Distribution of Duration of Excursions of Normal Fluctuations," *Radiotekhnika i Electronika*, Vol. 1, 1956, pp. 23–40; translated in *Non-Linear Transformations of Stochastic Processes*, Pergamon Press, New York, 1965, pp. 354–367.

[18] Rice J. R. and Beer, F. P., "First-Occurrence Time of High Level Crossings in a Continuous Random Process," *Journal of the Acoustical Society of America*, Vol. 39, 1966, pp. 323–335.

[19] Roberts, J. B., "Estimation of the Probability of First-Passage Failure for a Linear Oscillator," *Journal of Sound and Vibration*, Vol. 10, 1969, pp. 42–61.